HHS Public Access

Author manuscript

Nature. Author manuscript; available in PMC 2018 April 30.

Published in final edited form as:

Nature. 2017 November 23; 551(7681): 503–506. doi:10.1038/nature24474.

Synaptotagmin 7 confers frequency invariance onto specialized depressing synapses

Josef Turecek[1], **Skyler L. Jackman**[1], and **Wade G. Regehr**[2]

Department of Neurobiology, Harvard Medical School, 220 Longwood Avenue, Boston, Massachusetts 02115, USA

Abstract

At most synapses in the brain, short-term plasticity dynamically modulates synaptic strength. Rapid frequency-dependent changes in synaptic strength play critical roles in sensory adaptation, gain control and many other neural computations[1,2]. However, some auditory, vestibular and cerebellar synapses maintain constant strength over a wide range of firing frequencies[3–5], and as a result efficiently encode firing rates. Despite its apparent simplicity, frequency-invariant transmission is difficult to achieve because of inherent synaptic nonlinearities[6]. Here we study frequency-invariant transmission at Purkinje cell to deep cerebellar nuclear (PC to DCN) synapses and vestibular synapses. Prolonged activation of these synapses leads to initial depression, which is followed by steady-state responses that are frequency invariant for their physiological activity range. We find that Synaptotagmin 7 (Syt7), a recently identified calcium sensor for short-term facilitation[7], is present at both synapses. It was unclear why a sensor for facilitation would be present at these and other depressing synapses. We find that at PC and vestibular synapses, Syt7 supports a hidden component of facilitation that can be unmasked in wildtype animals but is absent in Syt7 knockout animals. In wildtype mice, facilitation increases with firing frequency and counteracts depression to produce frequency-invariant transmission. In Syt7 knockout mice, PC and vestibular synapses exhibit conventional use-dependent depression, weakening to a greater extent as the firing frequency is increased. Presynaptic rescue of Syt7 expression restores both facilitation and frequency-invariant transmission. Our results identify a function for Syt7 at synapses that exhibit overall depression, and demonstrate that facilitation plays an unexpected and important role in producing frequency-invariant transmission.

[2]Corresponding author: Wade Regehr, wade_regehr@hms.harvard.edu.

[1]Equal contribution

Contributions

J.T., S.J. and W.R. designed experiments. J.T. and S.J. performed electrophysiology. J.T. performed stereotaxic surgeries, immunohistochemistry and simulations. J.T. S.J. and W.R. wrote the manuscript.

Competing financial interests

The authors declare no competing financial interests.

Data availability

The data, computational models and analysis scripts that support the findings are available upon reasonable request of the corresponding author.

MAIN TEXT

A primary challenge to maintaining constant synaptic strength is that during high frequency presynaptic activation there is little time to replenish vesicles, and synaptic strength decreases as vesicle depletion becomes more severe (Extended Data Fig. 1a, b). Consequently, many synapses depress to a greater extent as activation frequencies increase[8–10]. This property can be used computationally as a dynamic gain control mechanism[1]. Despite the challenges posed by vesicle depletion, some synapses faithfully transmit across a wide range of activation frequencies[3–5] (Extended Data Fig. 1c–f). In the vestibular system, such frequency-invariant transmission effectively conveys the absolute firing rate of vestibular afferents, and contributes to the linearity of occulomotor reflexes[4]. Several mechanisms have been proposed to explain how synapses could maintain frequency-invariant transmission[3,5,11], but the molecular tools to address these models directly have remained elusive. Here we test the hypothesis that facilitation, a short-lived increase in the probability of release (P_R), counteracts vesicle depletion to produce frequency-invariant transmission (Extended Data Fig. 1d). We take advantage of the recent finding that genetic knockout of the slow synaptotagmin isoform Syt7 selectively eliminates facilitation at some synapses[7].

We began by studying synapses made by Purkinje cells (PCs), the sole output of the cerebellar cortex that fire spontaneously at 10 to 120 Hz in vivo[12]. PCs form GABAergic synapses in the deep cerebellar nuclei (DCN, Fig 1a), and express Syt7 (Fig 1b). The presence of Syt7 was intriguing because unlike many synapses with prominent Syt7 expression, PC to DCN synapses depress. We found that Syt7 expression at PC to DCN synapses is age dependent, which is not the case for the PC marker Calbindin and Syt2 (Extended Data Fig. 2). The onset of Syt7 expression is correlated with the development of frequency-invariant transmission at PC to DCN synapses (Fig 1c–f and Extended Data Fig. 3–4). In young animals Syt7 expression is low, and steady-state transmission is frequency-dependent in both wildtype and Syt7 knockouts (Fig $1c_1$–e_1). Syt7 expression increases in juvenile wildtype animals, and transmission becomes more frequency-invariant with age. However, in juvenile Syt7 knockouts frequency-invariant transmission does not develop (Fig. $1c_2$–e_2). The differences between wildtypes and knockouts become more pronounced in adults (Fig $1c_3$–e_3). As a consequence, synaptic charge transfer, the product of IPSC amplitude and activation frequency, becomes more linear during development in wildtype animals, but remains sublinear in Syt7 knockouts (Fig 1f). These findings indicate that Syt7 is required for frequency-invariant transmission at PC to DCN synapses.

To determine what caused the loss off frequency-invariant transmission in Syt7 knockouts, we examined recovery from depression, the initial release probability (P_R), and facilitation. It has been shown that Syt7 mediates rapid calcium-dependent recovery from depression in cultured hippocampal synapses[13]. One possibility is that Syt7 contributes to frequency-independent transmission by accelerating recovery from depression during high-frequency activity (Extended Data Fig. 1e). Recovery from depression would then be faster in wildtype animals than in Syt7 knockout animals, but this was not the case (Extended Data Fig. 5). Syt7 also mediates asynchronous release during high-frequency stimulation at some

synapses[14,15], but asynchronous release is not prominent at PC to DCN synapses (Extended Date Fig. 6).

We also tested the hypothesis that P_R is elevated in Syt7 knockout mice. If P_R were increased, stronger depletion could more effectively mask facilitation and lead to a loss of frequency-invariant transmission[6]. It is expected that an increase in P_R would increase the size of PC inputs, but we found no significant difference in single fiber size between wildtype and Syt7 knockouts (Extended Data Fig. 7). We lowered external calcium (Ca_e) to decrease P_R and reduced the masking effects of vesicle depletion, and found that at PC to DCN synapses facilitation was prominent in wildtypes, but weak or absent in Syt7 knockouts (Figure 2a). If the loss of frequency-independent transmission is a consequence of an increase in P_R, then reducing P_R by lowering Ca_e should lead to frequency-invariant transmission in Syt7 knockout animals. However, when Ca_e was lowered from 1.5 mM (control) to 1 or 0.5 mM to reduce IPSC amplitudes to 42% and 12% of control respectively[5], transmission in Syt7 knockout mice remained frequency-dependent (Fig 2b–c). These results indicate that the loss of frequency invariance in Syt7 knockout animals is not a consequence of an increase in initial P_R.

We next looked for evidence of facilitation in physiological Ca_e (1.5 mM). Facilitation was measured by first stimulating at 10 Hz to induce baseline depletion, followed by steps to 100 Hz[5,16]. In wildtype animals, frequency steps revealed a transient enhancement whose magnitude was correlated with the development of frequency-invariant transmission. (Fig $2d_{1–3}$). These results are consistent with facilitation leading to sustained increases in P_R that is transiently revealed until it is masked by vesicle depletion. In Syt7 knockout animals, facilitation was not observed at any age, and increases in stimulus frequency depressed IPSCs. Thus, Syt7-dependent facilitation is prominent when transmission is frequency independent (juveniles and adult wildtypes), and is weak when transmission is frequency dependent (young wildtype and Syt7 knockouts of all ages).

To determine whether impaired frequency-invariant transmission was due specifically to presynaptic loss of Syt7[17] we performed rescue experiments in global Syt7 knockout animals. We used AAVs to express ChR2-YFP alone, or to bicistronically express both Syt7 and ChR2-YFP presynaptically[7] (Fig. 3a). However, it is not possible to obtain expression in all PCs, and it is impractical to optically stimulate axons at high frequencies for prolonged trains[18]. We therefore used optical stimulation to identify ChR2-expressing fibers that could be isolated electrically (Fig. 3b, c). These axons were then electrically stimulated at high frequency. We found that in Syt7 knockouts facilitation was absent in axons expressing ChR2 alone, but was prominent in fibers expressing ChR2 and Syt7 (Fig. 3d). Steady-state transmission was nearly constant when Syt7 was expressed, but remained frequency-dependent when only ChR2 was present (Fig. 3e, f). Consequently, charge transfer in Syt7-expressing PC axons was linear, but remained sub-linear when only ChR2 was expressed (Fig. 3g–h). Viral expression of Syt7 allowed PCs in Syt7 knockouts to become as frequency invariant as wildtype animals (Fig. 3h), indicating that presynaptic Syt7 mediates frequency-invariant transmission.

Having established that Syt7 is required for frequency invariance in PC synapses, we asked whether Syt7 plays a similar role at vestibular synapses. Afferents from the vestibular ganglion project to the magnocellular medial vestibular nucleus (MVNm, Fig. 4a). Syt7 is expressed in the neuropil of the MVNm where vestibular afferents form glutamatergic synapses (Fig. 4b). Although previous studies did not report facilitation at this synapse[11], we found that vestibular synapses facilitate in low Ca_e in wildtype animals, but not in Syt7 knockouts (Fig. 4c). In physiological Ca_e, step changes in stimulation frequency produced transient enhancement in wildtypes but not in Syt7 knockouts(Fig. 4d). These responses suggest that at vestibular synapses Syt7-mediated facilitation is also present, but is masked by depletion. We also found that steady-state transmission was frequency-invariant and charge transfer was linear in wildtypes, but not in Syt7 knockouts (Fig. 4e–g, Extended Data Fig. 8).

Here we show that Syt7 mediates a hidden component of facilitation that counteracts partial vesicle depletion to produce linear charge transfer. Synaptic properties in wildtype and Syt7 knockouts conform to a model in which the loss of frequency-invariance in Syt7 knockouts is accounted for by the absence of facilitation[5] (Extended Date Figure 9). Linear charge transfer and Syt7 expression at PC synapses emerge during development, but for technical reasons most synapses have only been studied in young animals [19]. The prevalence of frequency-invariant transmission in adults is unknown but indirect measurements *in vivo* suggest it may be widespread[20,21]. Moreover, Syt7 is developmentally regulated[22,23] and widely expressed in the adult brain, often in cells that make depressing synapses[22,24]. The kinetics of Syt7 make it well suited to operate within the physiological firing range of PCs and vestibular afferents[4,12,25,26]. While our results show linear charge transfer is mediated by Syt7 at PC and vestibular synapses, other synapses may use different mechanisms (Extended Figure 1).

At frequency-invariant synapses, the amount of neurotransmitter release scales linearly with the firing frequency, and can thus faithfully encode presynaptic spike rates. Sensorimotor processing in the vestibular system and intensity discrimination in the auditory system have been proposed to operate through a linear rate code[4,273,28]. Understanding the mechanisms involved in frequency-invariant transmission will enable genetic manipulations that could yield fundamental insights into how synaptic computations contribute to circuit function and behavior.

Methods

Animals and viruses

All mice were handled in accordance with NIH guidelines and protocols approved by Harvard Medical Area Standing Committee on Animals. Syt7 knockout mice[42] (Jackson Laboratory) and wild-type littermates of either sex were used. Statistical tests were not used to predetermine sample size. In Figure 3–4, Extended Data Figure 2, 7, 8, all experiments were performed blind to genotype and virus identity. In Figures 1–2, Extended Data Figure 3–6, experiments were initially performed blind but abandoned after initial rounds of experiments because genotypes could easily be identified from physiology alone. AAV2/1-hSyn-hChR2(H134R)-EYFP was obtained from the University of Pennsylvania Vector Core.

AAV2/1-hSyn-hChR2(H134R)-EYFP-2A-Syt7 was obtained from the Boston Children's Virus Core. Plasmid sequences are available upon request. Stereotaxic surgeries were performed on P16-18 Syt7 knockout mice anesthetized with ketamine/xylazine (100/10 mg/kg) supplemented with isoflurane (1–4%). Viruses were injected through glass capillary needles using a Nanoject II (Drummond) mounted on a stereotaxic (Kopf). Three injections were made in the right cerebellar cortex, 1.0, 1.5, 2.0 mm lateral, 1 mm posterior from lambda, 0.2–0.3 mm depth. 300–500 nL of virus suspension was delivered to each site at a rate of 100 nL/minute, and the needle was retracted 5–10 minutes following injection. Analgesic (buprenorphine 0.05 mg/kg) was administered subcutaneously for 48 hours post-surgery.

Slice preparation

Acute slices were prepared in mice of both sexes (P21-32 unless otherwise indicated). Mice were sacrificed 12–14 days following AAV injections. Animals were anesthetized with ketamine/xylazine (100/10 mg/kg) and transcardially perfused with solution composed of in mM: 110 Choline Cl, 2.5 KCl, 1.25 NaH_2PO_4, 25 $NaHCO_3$, 25 glucose, 0.5 $CaCl_2$, 7 $MgCl_2$, 3.1 Na Pyruvate, 11.6 Na Ascorbate, 0.002 (R)-CPP, 0.005 NBQX, oxygenated with 95% O2 / 5% CO_2, kept at 35°C. For DCN recordings, a cut was made down the midline of the hindbrain, and the cut face of each side was glued to the slicing chamber to generate sagittal slices. For the vestibular nuclei, a cut was made down the midbrain between the cerebellum and cortex and glued to the slicing chamber to generate coronal slices. 250 μm thick sections were made on a Leica 1200S vibratome and were then transferred to a holding chamber with ACSF containing in mM: 127 NaCl, 2.5 KCl, 1.25 NaH_2PO_4, 25 $NaHCO_3$, 25 glucose, 1.5 $CaCl_2$, 1 $MgCl_2$, and allowed to recover at 35°C for at least 20 minutes before cooling to room temperature.

Electrophysiology

All experiments were performed at 34–35°C with a flow rate of 3–5 ml/min. Recording ACSF had the same composition as incubation ACSF unless otherwise stated. Recordings were made primarily in the dentate and interposed nuclei of the DCN. Large diameter (>15 μm) neurons were selected for recording as previously described [5]. For DCN recordings, borosilicate electrodes (1–2 MΩ) were filled with internal solution consisting in mM of: 110 CsCl, 10 HEPES, 10 TEA-Cl, 1 $MgCl_2$, 4 $CaCl_2$, 5 EGTA, 20 Cs-BAPTA, 2 QX314, 0.2 D600, pH to 7.3. Cells were held at −30 to −40 mV in the presence of 5 μM NBQX to block AMPARs, 2.5 μM (R)-CPP to block NMDARs, 1 μM strychnine to block glycine receptors, and 1 μM CGP 55845 to block $GABA_B$Rs. A glass monopolar stimulus electrode (2–3 MΩ) filled with ACSF was placed in the white matter surrounding the DCN to activate PC axons.

To study vestibular afferents, recordings were made from cells in the magnocellular medial vestibular nucleus. Recordings electrodes (1.5–2 MΩ) were filled with in mM: 150 Cs-gluconate, 3 CsCl, 10 HEPES, 0.5 EGTA, 3 MgATP, 0.5 NaGTP, 5 Tris-phosphocreatine-Tris and 5 Na-phosphocreatine; pH to 7.2. Cells were held at −60 mV in the presence of 100 μM picrotoxin or 5 μM SR-95531 to block $GABA_A$Rs, 2.5 μM (R)-CPP to block NMDARs, 1 μM strychnine to block glycine receptors, and 1 μM CGP 55845 to block $GABA_B$Rs. A concentric bipolar electrode was placed in the expansion of the vestibulocochlear nerve as it

reaches the dorsal brainstem, adjacent to the lateral vestibular nucleus. To prevent the possibility of poor fiber recruitment or entraining local circuit elements, trains with EPSCs composed of multi-phasic rise or decay phases were excluded from analysis. For trains in low Ca_e EPSCs became very small. In some cases, 5 μM NBQX was washed in at the end of experiments and traces in the presence of NBQX were subtracted in order to remove stimulus artifacts.

Trains of 100 stimuli (5–150 Hz, randomized), followed by 100 stimuli at 100 Hz, were applied every 20–30 s for vestibular and PC synapses. For 500 stimulus trains at 100 Hz, trials were collected every 60 s. Extracellular stimulation of axons became unreliable after 500 stimuli. For all recordings, only the capacitance roughly equivalent to the cell body was compensated (5 pF), and series resistance (1–6 MΩ) was compensated up to 80%. Experiments were discarded if series resistance changed by 30%. Experiments were discarded if fibers could not be consistently recruited, as assessed by major discrete changes observed in PSC amplitude during trains, or if the PSC amplitude never reached steady state during trains. Liquid junction potentials were left unsubtracted. In low Ca_e experiments, total divalents were kept constant by elevating external Mg. Experiments using the low affinity $GABA_AR$ antagonist TPMPA were performed as previously described[5].

Analysis

Recordings were collected using a Multiclamp 700B (Molecular Devices) in Igor Pro (Wavemetrics) sampled at 20 kHz and filtered at 4 kHz. All data was analyzed using custom-written scripts in Matlab (Mathworks). Stimulus artifacts were blanked for clarity. IPSC amplitudes during trains were measured from averaged traces of 3–10 trials as the peak evoked current, with a baseline measured 2 ms before stimulus onset. During high frequency trains, IPSCs did not fully decay before subsequent stimuli. Baselines in this case were measured by extrapolating a single exponential fit from the previous IPSC (as shown in Extended Data Figure 6). Trains from rest typically reached steady-state after 10–20 stimuli, and the steady-state was measured as the average IPSC size of the 40^{th} to the 60^{th} stimuli. Charge transfer was calculated as the product of steady-state IPSC size and stimulation frequency, and normalized to the charge transfer of 10 Hz stimulation. All data are presented as means ± s.e.m. unless otherwise indicated. In some cases error bars are occluded by markers. Statistical significance was assessed using unpaired two-tailed Student's t-test or one-way ANOVA with Tukey's post-hoc test unless otherwise noted. A subset of the data from wildtype Syt7 litter mate animals (~50%) in Figure 1 and Figure $2d_2$ was presented previously[5].

Optogenetics

It was impossible to reliably stimulate PC axons with prolonged trains at high frequency (>50 Hz) using optical stimulation alone (ChR2-H134R or Chronos). We therefore used ChR2 to identify labeled fibers that were then stimulated electrically. In this approach, optical stimulation of axons expressing ChR2 could occlude electrical stimulation of the same fibers, presumably because of the refractory period of the action potential. In contrast, if electrically stimulated fibers did not express ChR2, electrically-evoked responses could not be occluded by optical stimulation, and combined stimulation was equivalent to the

linear sum of optical and electrical activation alone. PC boutons expressing ChR2 were stimulated by pulses of 473 nm light (0.5–1 ms, 160 mW/mm^2) from an LED (Thorlabs) through a 60x objective producing an 80 μm diameter spot of light over the cell body. A stimulus electrode was placed in the white matter and converging PC axons were located as in other experiments. Randomized trials of single optical, electrical, or closely-timed (0–2 ms) paired optical/electrical stimuli were applied every 5 s. When >70% of the electrically evoked component could be occluded by optical stimulation, and could be consistently recruited, those fibers were then activated using high-frequency electrical stimulation. Following electrical trains, occlusion trials were performed again to confirm that the same set of fibers was stimulated throughout all trials. At the end of experiments, a low concentration of SR-95531 (300–800 nM) was washed in and occlusion trials were again repeated to ensure occlusion was not the result of poor voltage clamp. In a subset of experiments light pulses were also delivered over the stimulus electrode instead of the cell body, producing similar results.

Immunohistochemistry

Mice of both sexes (P21-32 unless otherwise indicated) were anesthetized with ketamine/xylazine (100/10 mg/kg) and transcardially perfused with PBS followed by 4% paraformaldehyde (PFA) in PBS. To determine the expression of Syt7, Syt2, Calbindin and VGAT specifically in PCs, we also perfused one mouse (P43) in which PC synapses are labeled with TdTomato (Pcp2-Cre(Jdhu) x Synaptophysin-TdTomato, Extended Data Fig. 2). Brains were removed and post-fixed in PFA overnight. Sagittal sections of the cerebellum or coronal sections of the brainstem (50 μm) were then permeabilized (0.2% triton X-100 in PBS) for 10 min and blocked for 1 hr (4% Normal Goat Serum in 0.1 % triton X-100) at room temperature. Slices were then incubated overnight at 4°C with primary antibodies (Mouse anti-Syt7 targeting the C2A domain, UC Davis/NIH NeuroMab Facility, clone N275/14, RRID: AB_11030371, 1 μg/mL, 1:100; Rabbit anti-Calbindin D28K, Millipore Ab1778, 1:200; Mouse anti-Syt2, Zirc znp-1, 1:200; Guinea-pig anti-VGAT, Synaptic Systems 131004, 1 μg/mL, 1:500; Guinea-pig anti-VGLUT2, Synaptic Systems 135404, 1 μg/mL, 1:1200). To prevent background when co-staining with VGLUT2 and Syt7, Syt7 primary antibodies were applied alone overnight at 4°C, then VGLUT2 primary antibodies alone for 2 hrs at room temperature. Following primaries, slices were incubated with secondary antibodies for 2 hrs at room temperature (anti-Rabbit-AlexaFluor488, Abcam ab150077; anti-Guinea-pig-AlexaFluor488, Abcam ab150185; anti-Mouse-AlexaFluor647, Abcam ab150115). For experiments comparing ages or genotypes, all tissue was stained and processed in parallel. Z-Stacks of each sample were collected using an Olympus Fluoview1000 confocal microscope using the same settings across ages and genotypes, and processed identically in ImageJ. For each genotype and age, identical anatomical locations and tissue depth were selected for presentation.

Modeling

In a previous study we modeled the PC to DCN synapse[5]. Models used previously to explain data in young animals[36] were reproduced, but could not fit data in P21-32 animals[5]. Several other types of models were also attempted but failed to accurately account for data observed in juvenile wildtype animals. We found that a two pool model fit all experimental

observations[5]. We extended this model to Syt7 knockout animals (Extended Figure 9). In this model there are 2 pools of vesicles, consisting of, respectively, N1 and N2 vesicles, initial probability of release P1 and P2 and time constants of recovery τ_{R1}, and τ_{R2}. P1 stays constant whereas P2 increases as a result of facilitation, F2, which has the frequency dependence that was determined experimentally. All of these parameters were constrained by extensive experimental studies for wildtype animals[5]. Once parameters for wildtype data were determined, F2 was set to 0 to model Syt7 knockout animals. Minor adjustments (<10% change) were made to some parameters to fit the data more accurately, with the exception of τ_{R1} which was reduced by 55% to conform to the observed recovery from depression in Syt7 knockouts (Extended Data Figure 5). This change in τ_{R1} had a negligible effect on steady-state IPSC amplitudes because Pool 1 still depletes rapidly. Parameters for modeling wildtypes were: N1/N2 = 0.35; P1 = 0.20; τ_{R1} = 7.7 s; P2 = 0.025; τ_{R2} = 0.2 s; F2 = 0.04; τ_{Fdeact} = 0.1 s. Parameters for modeling Syt7 knockouts were: N1/N2 = 0.36; P1 = 0.23; τ_{R1} = 3.5 s; P2 = 0.025; τ_{R2} = 0.2 s; F2 = 0.

Extended Data

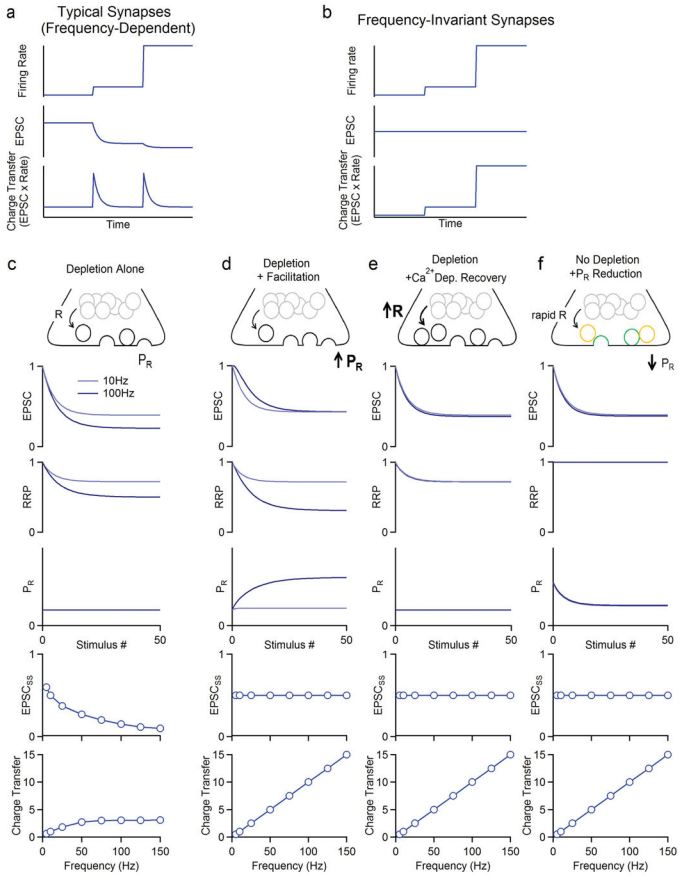

Extended Data Figure 1. Functions and possible mechanisms of frequency-invariant synapses

Short-term plasticity at synapses can be tuned to perform different computations. **a,** Many synapses in the brain undergo short-term depression that is use-dependent: elevations in presynaptic firing rate (top) result in more profound depression of post-synaptic currents

(EPSCs, middle). The charge transfer that ultimately drives post-synaptic firing rapidly increases with presynaptic firing, but short-term depression of the synapse reduces charge transfer back to a similar steady-state. Thus, short-term depression is suited to convey temporal information about changes in presynaptic firing. **b,** Some synapses maintain constant synapse strength across firing frequencies (top, middle). Charge transfer at these synapses therefore can reliably reflect the absolute rate of presynaptic firing. **c,** Typical depressing synapses can be well-approximated by intrinsic synaptic properties alone. Synapses have a limited number of vesicles in the readily releasable pool (RRP). High frequency presynaptic activity depletes the RRP until it can be replenished at some rate (R). Less recovery occurs as the interval between stimuli is reduced, thereby leading to an increase in depletion during high frequency stimulation. **d–f,** Other synaptic features must operate in order to generate frequency-invariant synapses, and several possibilities have been proposed. **d**, One way of making transmission frequency-invariant would be to balance depletion with facilitation[3,5] (Extended Data Figure 9). Activating a mechanism of short-term facilitation with high-frequency stimulation increases P_R, releasing more vesicles from the RRP. The increase in release results in steady-state transmission that is consistent across the physiological firing range. **e**, Another way of generating a frequency-invariant synapse is to have a rapid, calcium-dependent increase in R[29–33]. When the presynaptic frequency is elevated, presynaptic calcium and the rate of replenishment are increased to maintain the same RRP size regardless of activation frequency. However, this cannot explain the frequency invariance of PC and vestibular synapses, where recovery from depression is insensitive to stimulation frequency in juvenile animals[5,34]. **f**, A model proposed by McElvain et al.[34] proposes that each release site can hold two vesicles, but only one can be released per stimulus (green: releasable, orange: non-releasable). Vesicle replenishment to each release site is very rapid, and release is limited by decrease in P_R. Decreases in P_R are independent of stimulation frequency. The high replenishment rate and additional vesicle per release site results in very little vesicle depletion, and responses are instead shaped by decreases in P_R that are constant across frequencies. Another possibility is that a synapse could have very low P_R to limit vesicle depletion at each release site, but still maintain synaptic strength by having a very large number of release sites (not shown). However, such a mechanism would require an extremely large number of release sites, and is inconsistent with the depression present at PC and vestibular synapses. Finally, post-synaptic mechanisms of short-term plasticity, such as receptor saturation and desensitization, could also contribute to frequency-invariant transmission (not shown). These mechanisms are unlikely to contribute to frequency-invariance at PC and vestibular synapses because frequency-independent transmission is unaltered when saturation and desensitization are minimized by competitive low-affinity postsynaptic receptor antagonists[4,5].

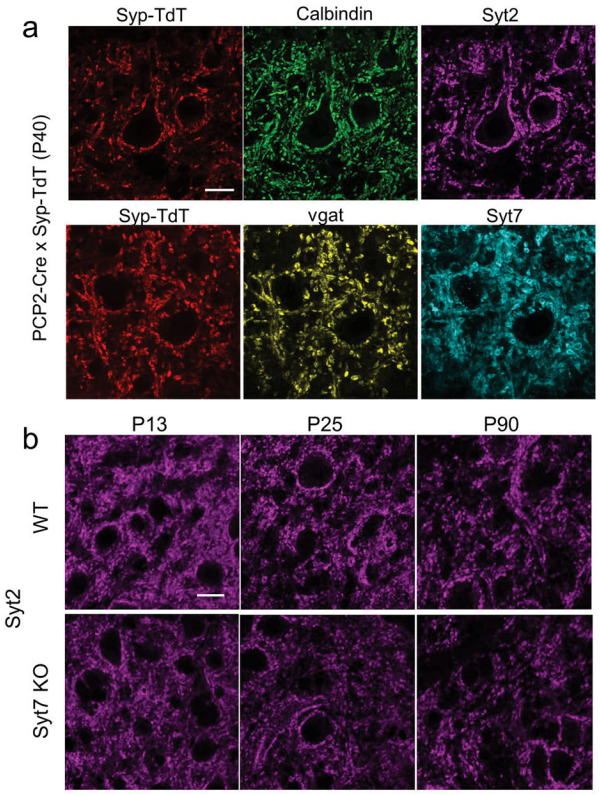

Extended Data Figure 2. Expression and localization of synaptic proteins to PC synapses in the DCN

To determine whether Syt7 was present in PC synapses in the DCN, we compared immunohistochemical labeling in mice expressing synaptophysin-TdTomato (Syp-TdT) specifically in PCs (PCP2-Cre x Syp-TdT). **a**, Syp-TdT could be observed in boutons surrounding neurons in the DCN (upper left). Immunolabeling of Calbindin could be seen in both PC boutons labeled with Syp-TdT, and throughout the length of PC axons traversing the DCN (upper middle). Syt2 was also highly expressed in PC boutons, with most Syt2 puncta co-localizing with Syp-TdT (upper right). We found that the vast majority of inhibitory synapses labeled by VGAT were syp-TdT positive, suggesting that most inhibitory input to the DCN arises from PCs (lower middle). Syt7 was also prominent in PC boutons labeled by Syp-TdT, but with less punctate expression compared to Syt2 or VGAT. Scale bar, 15 μm. **b,** The expression of Syt2 was stable across development, and showed no prominent differences in intensity between wildtypes and Syt7 knockouts. Scale bar, 20 μm.

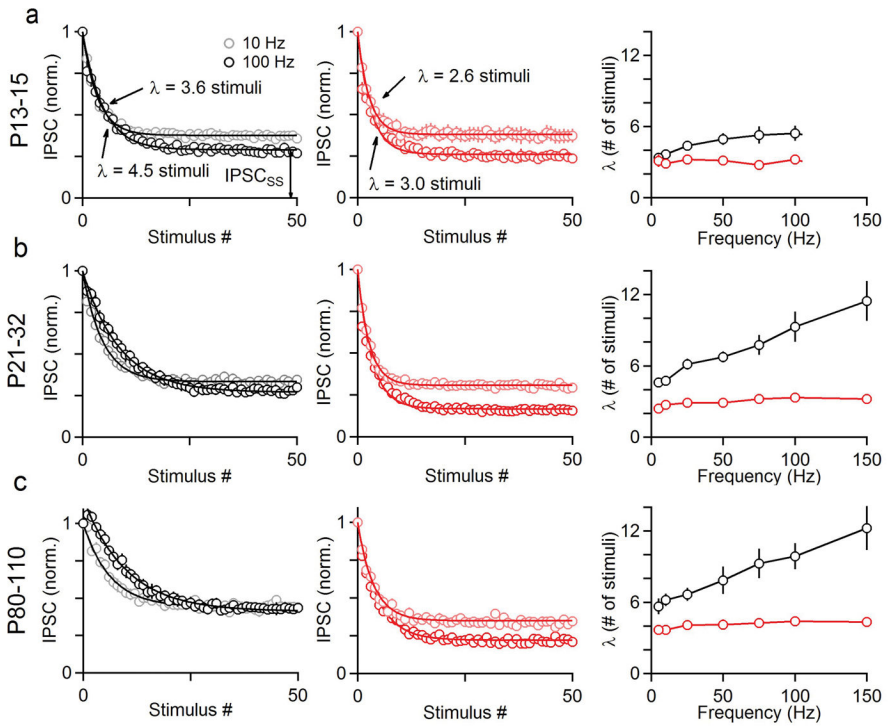

Extended Data Figure 3. Alterations in short-term depression at PC to DCN synapses in Syt7 knockout mice are consistent with the predicted consequences of eliminating facilitation

High frequency stimulation of the PC to DCN synapse leads to depressing IPSCs that can be approximated by the equation $IPSC = IPSC_{SS} + (1- IPSC_{SS})e^{-S/\lambda}$, where S is the stimulus number, $IPSC_{SS}$ is the steady-state IPSC amplitude, and λ is exponential decay constant. **a**, Average normalized IPSC amplitude for 10 and 100 Hz trains and fits in P13-15 wildtype (left) and Syt7 knockout (middle) mice. λ is plotted as a function of stimulation frequency (right). **b**, Same as in (**a**), but for P21-32 animals. **c**, Same as (**a**), but for P80-110 animals. According to a model of the PC to DCN synapse depression and facilitation are both present, but depletion of the readily releasable pool dominates and leads to depression during high frequency stimulation[5]. In wildtype animals λ is prolonged in a frequency-dependent manner, and it has been hypothesized that this arises from short-term facilitation that is more prominent as the stimulus frequency is increased. In young animals when Syt7 expression is low (Figure 1c), λ is weakly modulated by stimulation frequency. The prolongation of λ is more prominent in juveniles and adults. In the absence of Syt7, λ is not frequency dependent at any age. These observations are consistent with an age-dependent increase in Syt7 expression in wildtype animals leading to an age-dependent increase in facilitation, which in turn leads to age-dependent increases in the frequency dependence of λ. Data are mean ± s.e.m. Number of experiments shown in Extended Data Table 1.

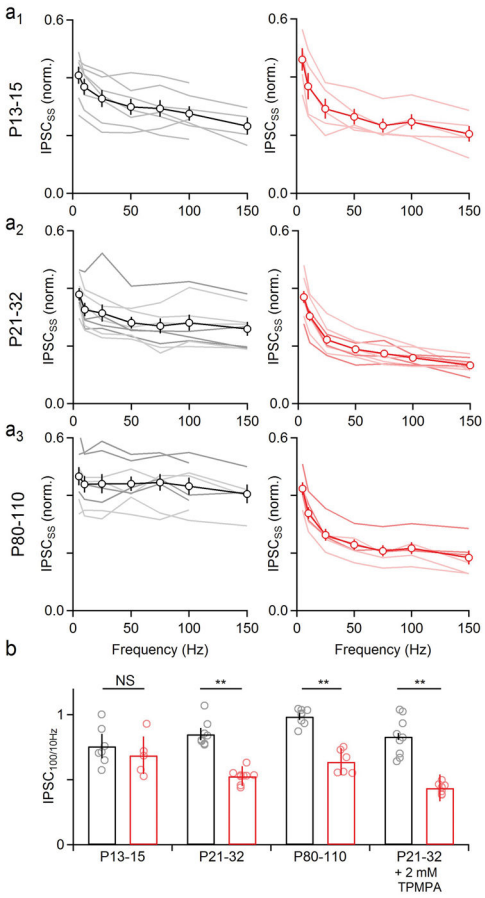

Extended Data Figure 4. The frequency dependence of synaptic strength is consistent for different cells for a given age and genotype

$a_{1–3}$, The steady-state IPSC amplitude as a function of frequency for each cell analyzed (thin lines) and averages (markers) for each genotype and age. Normalized steady-state IPSC amplitude across frequencies are plotted for wildtypes (left) and Syt7 knockouts (right) for P13-15 (**a_1**), P21-32 (**a_2**), and P80-110 (**a_3**) animals. **b,** Ratio of the steady-state IPSC amplitudes at 100 Hz divided by steady-state amplitudes at 10 Hz is summarized for different ages of wildtype and Syt7 knockouts, and in P21-32 animals in the presence of the low-affinity $GABA_AR$ antagonist TPMPA (2 mM, far right). Data from young animals is consistent with previous reports[5,35,36]. **p < 0.01, unpaired two-tailed Student's t-test. Data are mean ± s.e.m. Number of experiments shown in Extended Data Table 1.

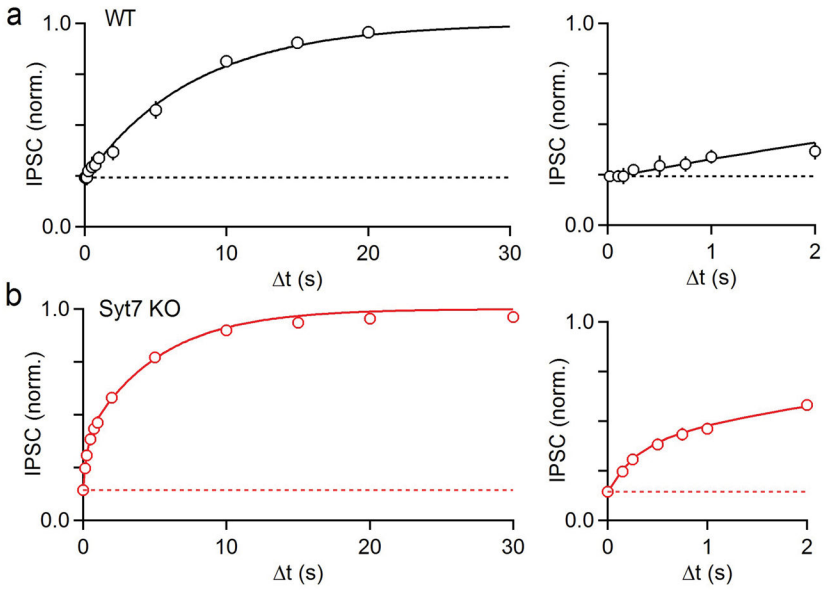

Extended Data Figure 5. Altered recovery from depression in Syt7 knockout mice cannot account for the loss of frequency invariance at the PC to DCN synapse in Syt7 knockout mice (P21-32)

It has been shown previously that the loss of Syt7 in hippocampal cultures slows recovery from depression[13]. If recovery from depression was slower in Syt7 knockouts, it could partially explain the reduction of sustained transmission at high frequencies. We therefore examined recovery from depression at PC to DCN synapses. One hundred stimuli at 100 Hz was followed by a single stimulus after an interval. This was repeated for many trials and a range of time intervals. Experiments were performed in wildtype (**a**) and Syt7 knockout (**b**) animals. **a,** PC to DCN synapses recovered slowly with a single exponential of 7.7 s (left). **b,** In Syt7 knockout mice recovery could not be approximated by a single exponential but was well approximated by a double exponential with time constants of 280 ms and 5.1 s. These findings indicate that a slowed recovery from depression does not occur in Syt7 knockout animals and thus does not contribute to the reduced steady-state responses in Syt7 knockout animals. The rapid time constant of recovery from depression that is apparent in Syt7 knockout animals is consistent with the prediction of a model of the PC to DCN synapse in which the decay of facilitation obscures this rapid phase of recovery in wildtype animals[5] (see Extended Fig. 9). The role of Syt7 in recovery from depression at the PC to DCN synapse differs from cultured hippocampal synapses where calcium dependent recovery from depression relies on Syt7, and recovery from depression is slowed in the absence of Syt7[13]. Data are mean ± s.e.m. Number of experiments shown in Extended Data Table 1.

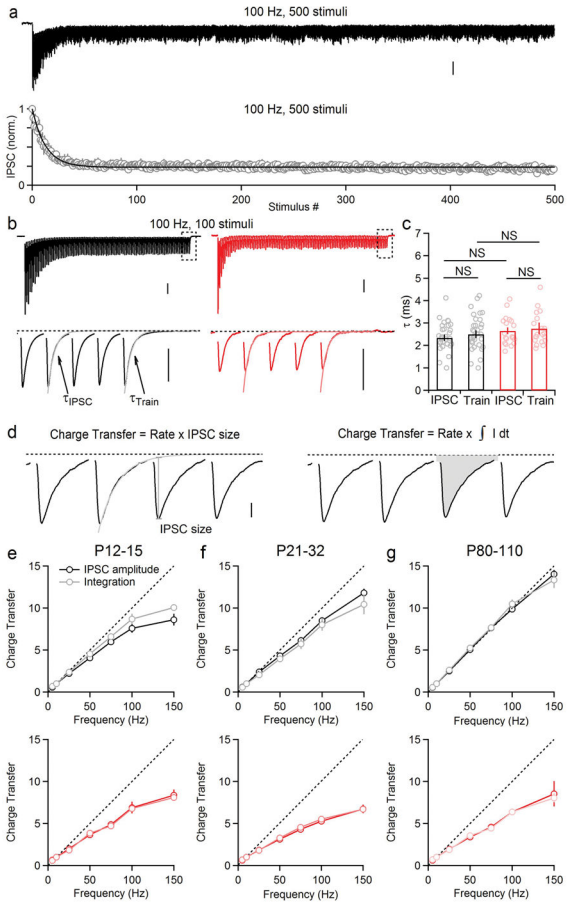

Extended Data Figure 6. Release from PCs to DCN neurons is sustained, fast and synchronous

a, PCs fire at high rates spontaneously in vivo. We therefore examined whether the PC to DCN synapse could sustain transmission for prolonged high frequency activation. **a**, Example of prolonged stimulation of PC axons (500 stimuli, 100 Hz), average of 4 trials (top), and average across cells (bottom) and fit with the equation IPSC = $IPSC_{SS}$ +(1−$IPSC_{SS}$)$e^{-S/\lambda}$ as in Extended Data Figure 3. Vertical scale bar, 1 nA. **b–g**, At some synapses asynchronous release becomes more prominent with prolonged high-frequency stimulation [14,15,37,38]. At these synapses, fast synchronous release can be seen riding on top of a slowly-decaying current that is in part mediated by asynchronous release. We therefore examined whether asynchronous release contributes to transmission during trains at this synapse. **b,** An example train of 100 stimuli at 100 Hz from a wildtype (black) and Syt7 knockout (red). We measured the average decay time constant of IPSCs during the train (average IPSC #50-99, τ_{IPSC}), and for the last IPSC in the train (τ_{Train}). IPSCs were well fit by a single exponential decay with similar τ's. This indicates that asynchronous release is not prominent at this synapse. Vertical scale bars, 0.5 nA, dashed line indicates baseline before the train. **c**, Average decay time for IPSCs during the train, and for the last IPSC in the train to decay back to baseline measured before the onset of stimulation. No significant differences were found between WT τ_{IPSC} vs WT τ_{train} (p = 0.36), KO τ_{IPSC} vs KO τ_{train} (p = 0.71), WT τ_{IPSC} vs KO τ_{IPSC} (p = 0.23), WT τ_{train} vs KO τ_{train} (p = 0.48), unpaired two-tailed student's t-test. **d**, Charge transfer was measured in two different ways to isolate

different components of release. The average incremental IPSC amplitude was multiplied by the stimulation rate (left), or traces were integrated and multiplied by stimulation rate (right). The average charge transfer as a function of stimulation frequency, calculated either by IPSC amplitude, or by integration, for **e,** young (P12-15), **f**, juvenile (P21-32), and **g**, adult (P80-110) wildtype and Syt7 knockouts is shown. Data are mean ± s.e.m. Number of experiments shown in Extended Data Table 1.

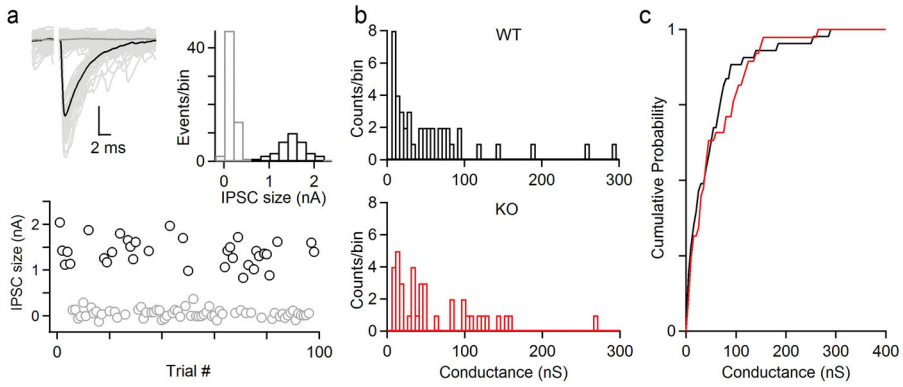

Extended Data Figure 7. Single fiber conductances are not elevated in Syt7 knockout mice (P21-32)

Single PC axons provide powerful inhibition on their post-synaptic targets in the DCN, and can be identified by their all-or-nothing nature. If the loss of Syt7 caused elevations in P_R, it would be expected to increase the strength of unitary fiber inputs. Experiments were done using minimal stimulation to determine the amplitudes of single PC to DCN inputs. **a**, The stimulus was adjusted so that at a constant intensity synaptic inputs were activated approximately half the time in a stochastic manner. This is shown for 100 superimposed traces (left), along with average of failures (thick grey) and average of successes (thick black), for the amplitude histogram for the events recorded in that cell (middle), and for the IPSC amplitude as a function of trial number (bottom). Vertical scale bar, 0.5 nA. **b,** Amplitude histogram of single fiber conductances for wildtype (black) and Syt7 knockouts (red). **c,** Cumulative amplitude histograms of single fiber conductances. No significant difference was found between wildtype and Syt7 knockouts. p = 0.43, Kolmogorov-Smirnov test. Number of experiments shown in Extended Data Table 1.

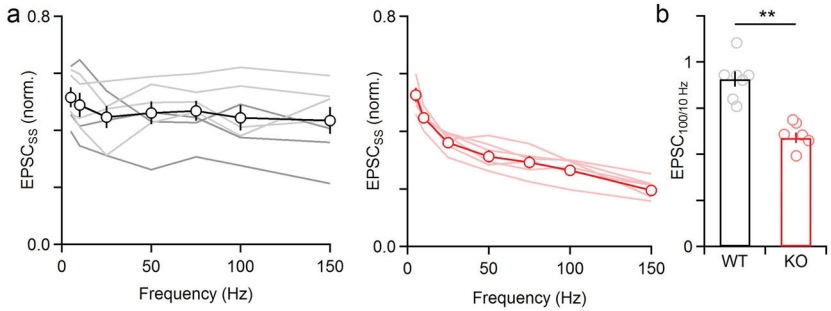

Extended Data Figure 8. The frequency invariance of synaptic strength is consistent in the MVNm

a, The steady-state EPSC size as a function of stimulation frequency for each cell analyzed (thin lines) and averages (markers) for wildtype (left, black) and Syt7 knockouts (red, right). **b,** Ratio of the steady-state EPSC amplitudes at 100 Hz divided by steady-state amplitudes at 10 Hz is summarized for vestibular synapses in wildtype and Syt7 knockouts. **p < 0.01, unpaired two-tailed Student's t-test. Data are mean ± s.e.m. Number of experiments shown in Extended Data Table 1.

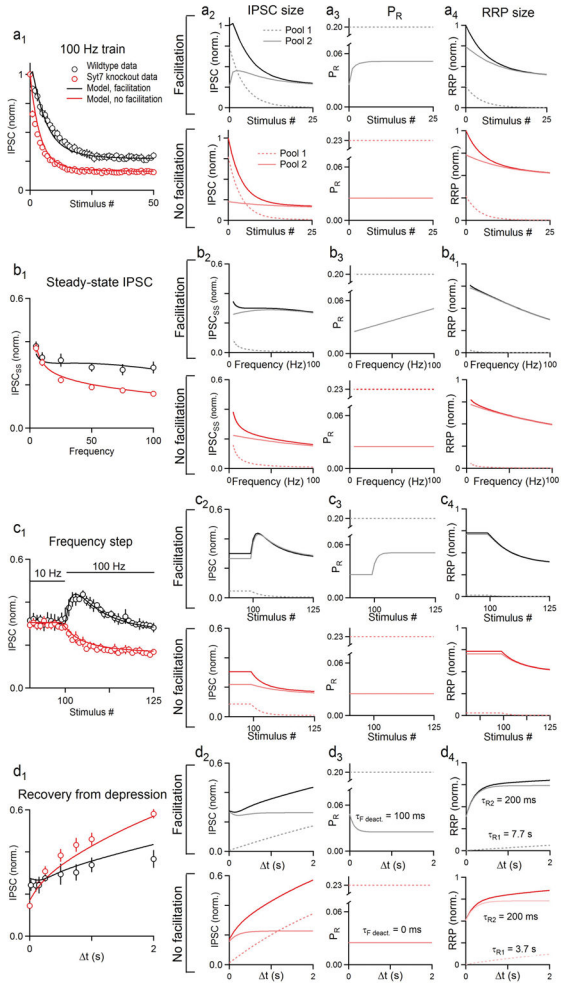

Extended Data Figure 9. A model of the PC to DCN synapses indicates that eliminating facilitation can explain the loss of frequency-invariant transmission and other synaptic changes observed in Syt7 knockout animals

We extended a previously described model of PC to DCN synapses to explore transmission in Syt7 knockout animals[5]. The model consists of two pools of vesicles: Pool 1 vesicles have a high release probability and are replenished slowly. Pool 2 vesicles have a low initial release probability that increases with facilitation (in wildtype animals only), and replenish rapidly. The existence of multiple vesicle pools has been proposed at several types of synapses[39–41]. The model was constrained by many experiments and in the simplest configuration could account for all experimental observations[5]. The model is compared to data in wildtype and Syt7 knockouts (**a_1–d_1**). The contribution of each pool and its

properties (IPSC size **a–d$_2$**, release probability P_R **a–d$_3$**, and readily releasable pool size RRP **a–d$_4$**) are also shown for each experiment. **a,** During high frequency stimulation in wildtype animals (**a$_{1–2}$,** black), Pool 1 primarily contributes to depression seen during the onset of stimulation, but is strongly depleted during sustained firing (**a$_2$**, dashed gray). Pool 2 facilitates and maintains release at steady-state (**a$_{2–3}$,** solid gray). We modeled Syt7 knockout animals by removing facilitation (**a$_3$,** red). When facilitation was eliminated, steady-state transmission was reduced during high frequency stimulation because fewer vesicles were released from Pool 2 (**a$_4$,** light red). **b,** In the model of wildtype synapses, the magnitude of facilitation increased with stimulation frequency (**b$_3$**, gray), allowing more of the readily releasable pool of Pool 2 (RRP2) to be released at high frequencies, resulting in similar IPSC amplitude across frequencies (**b$_{1–2}$**, black). When facilitation was removed (**b$_3$,** red), transmission was no longer frequency invariant, because fewer vesicles were released at high frequencies (**b$_{1,4}$,** red). **c**, When the frequency of stimulation was stepped from 10 to 100 Hz, a transient enhancement was observed in wildtype animals (**c$_1$**, black markers). In the model, this transient enhancement is mediated by facilitation of Pool 2 (**c$_3$,** gray). Facilitation is weakly activated by 10 Hz stimulation, but increases when stepping to 100 Hz stimulation. As more vesicles are released, RRP2 is partially depleted and the IPSC amplitude depresses, ultimately reaching steady-state levels that are similar to those reached during 10 Hz stimulation. When facilitation is removed, no transient enhancement occurs, and the IPSC amplitude simply depresses (**c$_{1–2}$,** red). **d**, The model is also able to explain recovery from depression. In wildtype animals, a single slow recovery is observed (**d$_1$**, black markers) because the decay of facilitation obscures the rapid recovery of RRP2 (**d$_{3–4}$**, τ_{Fdeact}). When facilitation is removed, this rapid component of recovery is unmasked (**d$_{1–2}$**, red). The known role of Syt7 in facilitation, and the fact that the many alterations in synaptic responses in Syt7 knockout animals are explained by eliminating facilitation in this model, support the importance of Syt7-mediated facilitation in frequency invariant transmission.

Extended Data Table 1

Number of electrophysiological recordings from WT and syt7 KO animals.

Figure	Experiment	Age	Genotype	Cells	Animals
Figure 1e$_1$–f$_1$, Extended Data 3a, 4a$_1$, 6e	Trains (5–150 Hz)	P13-15	wildtype	7	3
			Syt7 knockout	5	2
Figure 1e$_2$–f$_2$, Figure 3h Extended Data 3b, 4a$_2$, 6f	Trains (5–150 Hz)	P21-32	wildtype	9	8
			Syt7 knockout	9	8
Figure 1e$_3$–f$_3$, Extended Data 3c, 4a$_3$, 6g	Trains (5–150 Hz)	P80-110	wildtype	8	5
			Syt7 knockout	6	2
Extended Data 4b	Trains (5–150 Hz) in 2 mM TPMPA	P21-32	wildtype	9	6
			Syt7 knockout	7	5
Extended Data 5	Recovery from depression (100 Hz)	P21-32	wildtype	6	5
			Syt7 knockout	6	4
Extended Data 6	Long train (500 stimuli, 100 Hz)	P21-32	wildtype	4	2
Extended Data 6	IPSC kinetics (τ_{IPSC}, τ_{train})	P21-32	wildtype	32	22

Figure	Experiment	Age	Genotype	Cells	Animals
			Syt7 knockout	12	8
Extended Data 7	Single PC fibers	P21-32	wildtype	44 (# fibers)	6
			Syt7 knockout	37 (# fibers)	7
Figure 2b,	0.3 mM Ca_e Trains (100 Hz)	P21-32	wildtype	5	2
			Syt7 knockout	5	3
Figure 2c,	0.5 mM Ca_e Trains (5–100 Hz)	P21-32	wildtype	6	5
			Syt7 knockout	4	3
Figure 2c,	1.0 mM Ca_e Trains (5–100 Hz)	P21-32	wildtype	4	3
			Syt7 knockout	4	4
Figure $2d_1$	Frequency step (10–100 Hz)	P13-15	wildtype	4	3
			Syt7 knockout	5	2
Figure $2d_2$	Frequency step (10–100 Hz)	P21-32	wildtype	5	4
			Syt7 knockout	9	8
Figure $2d_3$	Frequency step (10–100 Hz)	P80-110	wildtype	6	5
			Syt7 knockout	6	2
Figure 3b–h	Optical occlusion Frequency step (10–100 Hz) Trains (5–100 Hz)	P21-32	KO+ChR2	7	3
			KO+ChR2+Syt7	5	5
Figure 4c	0.5 mM Ca_e Trains (100 Hz)	P21-32	wildtype	6	3
			Syt7 knockout	6	2
Figure 4d–f Extended Data 8	Frequency step (10–100 Hz) Trains (5–100 Hz)	P21-32	wildtype	7	6
			Syt7 knockout	6	2

Acknowledgments

We thank P. Kaeser and the Regehr lab for comments on the manuscript. This work was supported by grants from the NIH (R01NS032405 and R35NS097284) and a Nancy Lurie Marks grant to W.R., the Vision Core and NINDS P30 Core Center grant (NS072030) to the Neurobiology Imaging Center at Harvard Medical School and a Nancy Lurie Marks Fellowship to S.L.J.

References

1. Abbott LF, Varela JA, Sen K, Nelson SB. Synaptic depression and cortical gain control. Science. 1997; 275:220–224. [PubMed: 8985017]
2. Abbott LF, Regehr WG. Synaptic computation. Nature. 2004; 431:796–803. DOI: 10.1038/nature03010 [PubMed: 15483601]
3. MacLeod KM, Horiuchi TK, Carr CE. A role for short-term synaptic facilitation and depression in the processing of intensity information in the auditory brain stem. Journal of neurophysiology. 2007; 97:2863–2874. DOI: 10.1152/jn.01030.2006 [PubMed: 17251365]
4. Bagnall MW, McElvain LE, Faulstich M, du Lac S. Frequency-independent synaptic transmission supports a linear vestibular behavior. Neuron. 2008; 60:343–352. DOI: 10.1016/j.neuron.2008.10.002 [PubMed: 18957225]
5. Turecek J, Jackman SL, Regehr WG. Synaptic Specializations Support Frequency-Independent Purkinje Cell Output from the Cerebellar Cortex. Cell reports. 2016; 17:3256–3268. DOI: 10.1016/j.celrep.2016.11.081 [PubMed: 28009294]

6. Zucker RS, Regehr WG. Short-term synaptic plasticity. Annual review of physiology. 2002; 64:355–405. DOI: 10.1146/annurev.physiol.64.092501.114547
7. Jackman SL, Turecek J, Belinsky JE, Regehr WG. The calcium sensor synaptotagmin 7 is required for synaptic facilitation. Nature. 2016; 529:88–91. DOI: 10.1038/nature16507 [PubMed: 26738595]
8. Cook DL, Schwindt PC, Grande LA, Spain WJ. Synaptic depression in the localization of sound. Nature. 2003; 421:66–70. DOI: 10.1038/nature01248 [PubMed: 12511955]
9. Galarreta M, Hestrin S. Frequency-dependent synaptic depression and the balance of excitation and inhibition in the neocortex. Nature neuroscience. 1998; 1:587–594. DOI: 10.1038/2882 [PubMed: 10196566]
10. Brenowitz S, David J, Trussell L. Enhancement of synaptic efficacy by presynaptic GABA(B) receptors. Neuron. 1998; 20:135–141. [PubMed: 9459449]
11. McElvain LE, Faulstich M, Jeanne JM, Moore JD, du Lac S. Implementation of linear sensory signaling via multiple coordinated mechanisms at central vestibular nerve synapses. Neuron. 2015; 85:1132–1144. DOI: 10.1016/j.neuron.2015.01.017 [PubMed: 25704949]
12. Zhou H, et al. Cerebellar modules operate at different frequencies. eLife. 2014; 3:e02536. [PubMed: 24843004]
13. Liu H, et al. Synaptotagmin 7 functions as a Ca2+-sensor for synaptic vesicle replenishment. eLife. 2014; 3:e01524. [PubMed: 24569478]
14. Wen H, et al. Distinct roles for two synaptotagmin isoforms in synchronous and asynchronous transmitter release at zebrafish neuromuscular junction. Proc Natl Acad Sci U S A. 2010; 107:13906–13911. [PubMed: 20643933]
15. Luo F, Sudhof TC. Synaptotagmin-7-Mediated Asynchronous Release Boosts High-Fidelity Synchronous Transmission at a Central Synapse. Neuron. 2017; 94:826–839e823. DOI: 10.1016/j.neuron.2017.04.020 [PubMed: 28521135]
16. Muller M, Goutman JD, Kochubey O, Schneggenburger R. Interaction between facilitation and depression at a large CNS synapse reveals mechanisms of short-term plasticity. The Journal of neuroscience: the official journal of the Society for Neuroscience. 2010; 30:2007–2016. DOI: 10.1523/JNEUROSCI.4378-09.2010 [PubMed: 20147529]
17. Wu D, et al. Postsynaptic synaptotagmins mediate AMPA receptor exocytosis during LTP. Nature. 2017; 544:316–321. DOI: 10.1038/nature21720 [PubMed: 28355182]
18. Jackman SL, Beneduce BM, Drew IR, Regehr WG. Achieving high-frequency optical control of synaptic transmission. The Journal of neuroscience: the official journal of the Society for Neuroscience. 2014; 34:7704–7714. DOI: 10.1523/JNEUROSCI.4694-13.2014 [PubMed: 24872574]
19. Borst JG. The low synaptic release probability in vivo. Trends in neurosciences. 2010; 33:259–266. DOI: 10.1016/j.tins.2010.03.003 [PubMed: 20371122]
20. Arenz A, Silver RA, Schaefer AT, Margrie TW. The contribution of single synapses to sensory representation in vivo. Science. 2008; 321:977–980. DOI: 10.1126/science.1158391 [PubMed: 18703744]
21. Kuenzel T, Borst JG, van der Heijden M. Factors controlling the input-output relationship of spherical bushy cells in the gerbil cochlear nucleus. The Journal of neuroscience: the official journal of the Society for Neuroscience. 2011; 31:4260–4273. DOI: 10.1523/JNEUROSCI.5433-10.2011 [PubMed: 21411667]
22. Sugita S, et al. Synaptotagmin VII as a plasma membrane Ca(2+) sensor in exocytosis. Neuron. 2001; 30:459–473. [PubMed: 11395007]
23. Bakken TE, et al. A comprehensive transcriptional map of primate brain development. Nature. 2016; 535:367–375. DOI: 10.1038/nature18637 [PubMed: 27409810]
24. Lein ES, et al. Genome-wide atlas of gene expression in the adult mouse brain. Nature. 2007; 445:168–176. DOI: 10.1038/nature05453 [PubMed: 17151600]
25. Jackman SL, Regehr WG. The Mechanisms and Functions of Synaptic Facilitation. Neuron. 2017; 94:447–464. DOI: 10.1016/j.neuron.2017.02.047 [PubMed: 28472650]
26. Brandt DS, Coffman MD, Falke JJ, Knight JD. Hydrophobic contributions to the membrane docking of synaptotagmin 7 C2A domain: mechanistic contrast between isoforms 1 and 7. Biochemistry. 2012; 51:7654–7664. DOI: 10.1021/bi3007115 [PubMed: 22966849]

27. Robinson DA. The use of control systems analysis in the neurophysiology of eye movements. Annual review of neuroscience. 1981; 4:463–503. DOI: 10.1146/annurev.ne.04.030181.002335
28. Sullivan WE, Konishi M. Segregation of stimulus phase and intensity coding in the cochlear nucleus of the barn owl. The Journal of neuroscience: the official journal of the Society for Neuroscience. 1984; 4:1787–1799. [PubMed: 6737041]
29. Sakaba T, Neher E. Calmodulin mediates rapid recruitment of fast-releasing synaptic vesicles at a calyx-type synapse. Neuron. 2001; 32:1119–1131. [PubMed: 11754842]
30. Dittman JS, Regehr WG. Calcium dependence and recovery kinetics of presynaptic depression at the climbing fiber to Purkinje cell synapse. The Journal of neuroscience: the official journal of the Society for Neuroscience. 1998; 18:6147–6162. [PubMed: 9698309]
31. Stevens CF, Wesseling JF. Activity-dependent modulation of the rate at which synaptic vesicles become available to undergo exocytosis. Neuron. 1998; 21:415–424. [PubMed: 9728922]
32. Wang LY, Kaczmarek LK. High-frequency firing helps replenish the readily releasable pool of synaptic vesicles. Nature. 1998; 394:384–388. DOI: 10.1038/28645 [PubMed: 9690475]
33. Yang H, Xu-Friedman MA. Impact of synaptic depression on spike timing at the endbulb of Held. Journal of neurophysiology. 2009; 102:1699–1710. DOI: 10.1152/jn.00072.2009 [PubMed: 19587324]
34. McElvain LE, Bagnall MW, Sakatos A, du Lac S. Bidirectional plasticity gated by hyperpolarization controls the gain of postsynaptic firing responses at central vestibular nerve synapses. Neuron. 2010; 68:763–775. DOI: 10.1016/j.neuron.2010.09.025 [PubMed: 21092864]
35. Telgkamp P, Raman IM. Depression of inhibitory synaptic transmission between Purkinje cells and neurons of the cerebellar nuclei. The Journal of neuroscience: the official journal of the Society for Neuroscience. 2002; 22:8447–8457. [PubMed: 12351719]
36. Telgkamp P, Padgett DE, Ledoux VA, Woolley CS, Raman IM. Maintenance of high-frequency transmission at purkinje to cerebellar nuclear synapses by spillover from boutons with multiple release sites. Neuron. 2004; 41:113–126. [PubMed: 14715139]
37. Atluri PP, Regehr WG. Delayed release of neurotransmitter from cerebellar granule cells. The Journal of neuroscience: the official journal of the Society for Neuroscience. 1998; 18:8214–8227. [PubMed: 9763467]
38. Hefft S, Jonas P. Asynchronous GABA release generates long-lasting inhibition at a hippocampal interneuron-principal neuron synapse. Nature neuroscience. 2005; 8:1319–1328. DOI: 10.1038/nn1542 [PubMed: 16158066]
39. Lu HW, Trussell LO. Spontaneous Activity Defines Effective Convergence Ratios in an Inhibitory Circuit. The Journal of neuroscience: the official journal of the Society for Neuroscience. 2016; 36:3268–3280. DOI: 10.1523/JNEUROSCI.3499-15.2016 [PubMed: 26985036]
40. Trommershauser J, Schneggenburger R, Zippelius A, Neher E. Heterogeneous presynaptic release probabilities: functional relevance for short-term plasticity. Biophysical journal. 2003; 84:1563–1579. DOI: 10.1016/S0006-3495(03)74967-4 [PubMed: 12609861]
41. Thanawala MS, Regehr WG. Determining synaptic parameters using high-frequency activation. J Neurosci Methods. 2016; 264:136–152. DOI: 10.1016/j.jneumeth.2016.02.021 [PubMed: 26972952]
42. Chakrabarti S, et al. Impaired membrane resealing and autoimmune myositis in synaptotagmin VII-deficient mice. The Journal of cell biology. 2003; 162:543–549. DOI: 10.1083/jcb.200305131 [PubMed: 12925704]

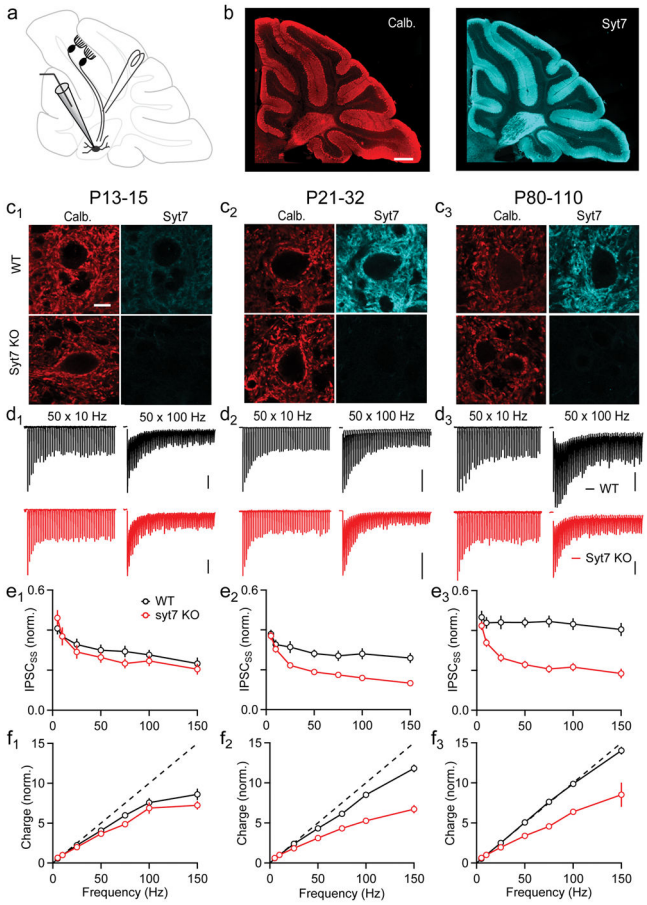

Figure 1. Syt7 is required for frequency-invariant transmission at PC to DCN synapses

a, PC axons were stimulated and responses were recorded from DCN projection neurons. **b**, Sagittal cerebellum from a P25 wildtype mouse immunolabeled for Calbindin and Syt7. Scalebar, 0.5 mm. **c**, High-power images of the DCN immunolabeled for Calbindin and Syt7 shown for young (**c_1**, P13-15), juvenile (**c_2**, P21-32), and adult (**c_3**, P80-110) wildtype and Syt7 knockouts. Scalebar, 10 μm**. d**, Representative IPSCs for wildtype (black) and Syt7 knockouts (red). Vertical scalebars, 1 nA. **e**, Normalized steady-state amplitudes ($IPSC_{SS}$) as a function of stimulation frequency for young (**e_1**), juveniles (**e_2**) and adults (**e_3**). **f**, Charge transfer calculated as the product of $IPSC_{SS}$ amplitude and stimulation frequency for young (**f_1**), juveniles (**f_2**) and adults (**f_3**). Data are mean ± s.e.m. Number of experiments in Extended Data Table 1.

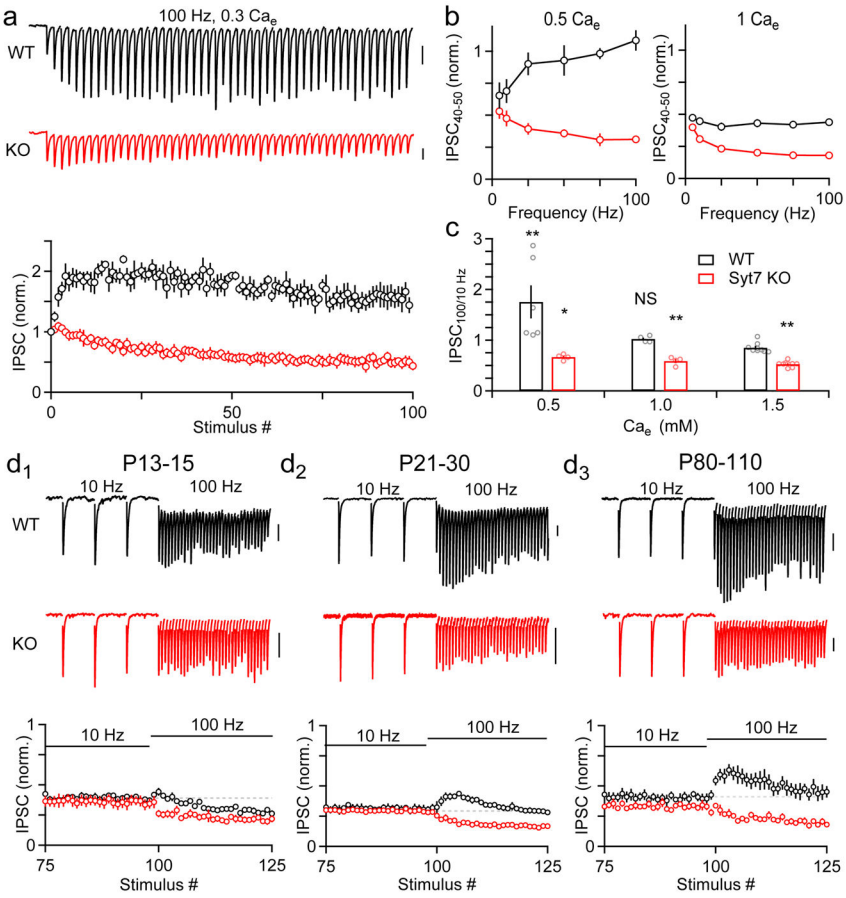

Figure 2. Syt7 is required for a hidden form of facilitation at PC to DCN synapses

a, Experiments were conducted in P21-32 mice in low Ca_e (0.3 mM) to reduce the initial probability of release. Responses are shown for representative experiments (top) and summarized across experiments (bottom). **b**, Average of 40–50th IPSC as a function of stimulation frequency. **c**, Ratio of $IPSC_{SS}$ from 100 and 10 Hz stimulation in different Ca_e. **$d_{1–3}$**, PC synapses were stimulated in 1.5 mM Ca_e at 10 Hz to reach steady-state, followed by 100 Hz stimulation in young (**d_1**) juvenile (**d_2**) and adult (**d_3**) animals. Example responses (top) and summaries (bottom) are shown. Vertical scale bars, 0.25 nA. *p < 0.05, **p < 0.01, one-way ANOVA with Tukey's post-hoc test. Data are mean ± s.e.m. Number of experiments in Extended Data Table 1.

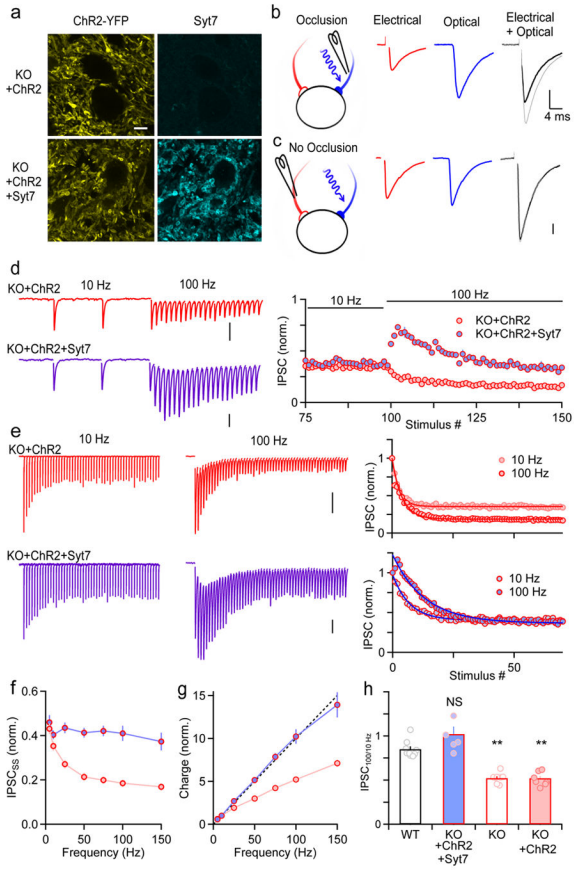

Figure 3. Presynaptic expression of Syt7 restores facilitation and frequency-invariant transmission at PC to DCN synapses in Syt7 knockouts

a, ChR2-YFP fluorescence and Syt7 immunolabeling in the DCN of Syt7 knockouts following AAV-driven expression of either ChR2-YFP alone (a, top) or ChR2-YFP and Syt7 (a, bottom) in PCs. Scalebar, 10 μm. **b, c**, The ability of IPSCs evoked electrically and optically to occlude each other was used to identify labeled fibers. **b**, If PC fibers express ChR2, the algebraic sum of electrical (red) and optical (blue) stimulation (gray) exceeds responses evoked by simultaneous optical/electrical stimulation (black). **c**, If electrically stimulated axons did not express ChR2, the sum of optical and electrical responses (gray) matched responses evoked by simultaneous optical and electrical stimulation (black). **d**, PC axons expressing ChR2 alone (red) or ChR2+Syt7 (purple) were electrically stimulated at 10 Hz and then 100 Hz e. **e–g**, PC inputs were stimulated at 5–150 Hz for ChR2 alone (red) or ChR2+ Syt7 (purple). **e**, Responses evoked by trains. Vertical scale bars, 1 nA. **f**, Average steady-state responses vs. stimulation frequency. **g,** Charge transfer as a function of stimulation frequency. **h,** Summary of ratios of $IPSC_{SS}$ amplitudes at 100 Hz and 10 Hz. **p < 0.01, one-way ANOVA with Tukey's post-hoc test. Data are mean ± s.e.m. Number of experiments in Extended Data Table 1.

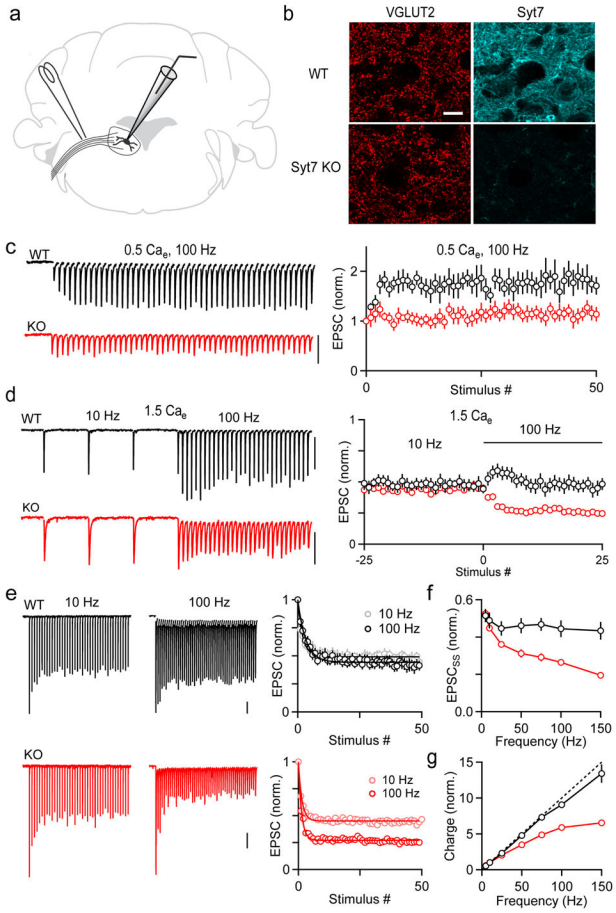

Figure 4. Syt7 is also required for frequency-invariant transmission at vestibular synapses

a, Schematic showing stimulus electrode placement to activate vestibular afferents while recording from MVNm neurons. **b**, Immunofluorescence of VGLUT2 (left) and Syt7 (right) surrounding MVNm cells in P25 mice. **c**, Responses evoked by stimulating vestibular afferents in 0.5 mM Ca_e. **d,** Vestibular inputs were stimulated at 10 Hz, followed by 100 Hz in 1.5 mM Ca_e. **e–g**, Vestibular inputs were stimulated with 5–150 Hz trains in 1.5 mM Ca_e for wildtype and Syt7 knockout mice. **e**, Responses evoked by trains are shown. **f**, Average steady-state responses vs. stimulation frequency. **g,** Charge transfer as a function of stimulation frequency. Vertical scale bars, 0.1 nA. Data are mean ± s.e.m. Number of experiments in Extended Data Table 1.